

Application of the Experimental Planning Design to the Notched Precracked Tensile Fracture of Composite

N. Mahmoudi

Abstract—Composite materials have important assets compared to traditional materials. They bring many functional advantages: lightness, mechanical resistance and chemical, etc. In the present study we examine the effect of a circular central notch and a precrack on the tensile fracture of two woven composite materials. The tensile tests were applied to a standardized specimen, notched and a precracked (orientation of the crack 0° , 45° and 90°). These tensile tests were elaborated according to an experimental planning design of the type 23.31 requiring 24 experiments with three repetitions. By the analysis of regression, we obtained a mathematical model describing the maximum load according to the influential parameters (hole diameter, precrack length, angle of a precrack orientation). The specimens precracked at 90° have a better behavior than those having a precrack at 45° and still better than those having of the precracks oriented at 0° . In addition the maximum load is inversely proportional to the notch size.

Keywords—Polymer matrix, Glasses, Fracture.

I. INTRODUCTION

FRACTURE mechanics finds extensive applications in damage analysis of composite laminates. In all materials, brittle or ductile, homogeneous or composites, fracture is governed more or less by microscopic discontinuities and imperfections, such as cracks, inclusions, or dispersed phases. The material strength may be correlated with its fracture energy, elastic modulus, and the size of the crack initiating the fracture. The importance of estimating the fracture load of notched plates is more or less established while influence of related parameters like notch geometry, thickness of specimen, notch angle, and notch dept are widely studied [1]. One of the most important parameters in the application of fracture mechanics in composite structures is the energy release rate. Composite materials offer some exciting advantages over more traditional metallic materials. Applications range from ski sticks, tennis rackets and reinforcement of highway bridges to advanced aircraft and space vehicles. More widely, diverse applications suffer from difficulties in recycling to questions of long term durability and the inability to predict their life accurately.

In order to predict the life of the structural integrity of composite components, designers must possess a good understanding of the effect of stress concentrations around design features. The problem of predicting the notched strength of composite materials is one that has attracted a great

deal of research over a period of around 30 years. There are a few studies concerning failure of notched woven fabric composite in literature. Naik et al. [2], Xiao et al. [3] and Kim et al. [4] demonstrated the applicability of the Whitney-Nuismer models. Damage development and fracture in notched woven fabric composites is affected by the range of variables, in particular notch size and shape, laminate lay-up and thickness. In the fracture field, Ashbee et al. [5] have verified, in an experimental way, the micromechanical damage due to cracking between inter-phase and matrix in composite. The present paper is concerned with the experimental characterization of the notched tensile fracture of two woven fabric composite materials. The notched and precracked specimens were subjected to the tensile tests in order to obtain the maximum fracture loads. A precrack was realised for a different length and orientation (0° , 45° and 90°). Applying the experimental design planning, a model describing the effect of all parameters was obtained.

II. MATERIALS

Two woven fabric composite materials were investigated. They were made of two panels of 350mm x 350mm, with a nominal thickness of 2 mm. The commercial denominations for these materials are RT270 and RT440. The panels were made of a bidirectional woven RT270 and RT440 glass fibre see Fig. 1 (with an unsaturated polyester thermoplastic matrix). The weight fraction of matrix considered was 30% for both materials. The laminates were made of 7 layers for RT270 and 4 layers for RT440.

III. PREPARATION OF SPECIMENS

The specimens were moulded first at 2 Bar and 315°C for 20 min and then at 20 Bar and 140°C for 10 min. The specimens were cut according to ASTM D3039 [6], and Tab aluminium end tabs were stuck on both sides of the specimens using 3M adhesive. The dimensions of the specimens were 125 x 20 x 2mm. Circular central holes with 2, and 4mm diameters were drilled. For each diameter, artificial precracks with length 1, 2 and 3mm were realized. The precracks orientation angles were 0° , 45° and 90° for each length and diameter. The precracks were perpendicular to the loading axis and carried out on one side of the circumference.

N. Mahmoudi is with the Laboratoire genie industriel et developpement durable, Centre Universitaire Relizane, Algeria (phone:+213561557999; e-mail: mahmoudi.nord@gmail.com).

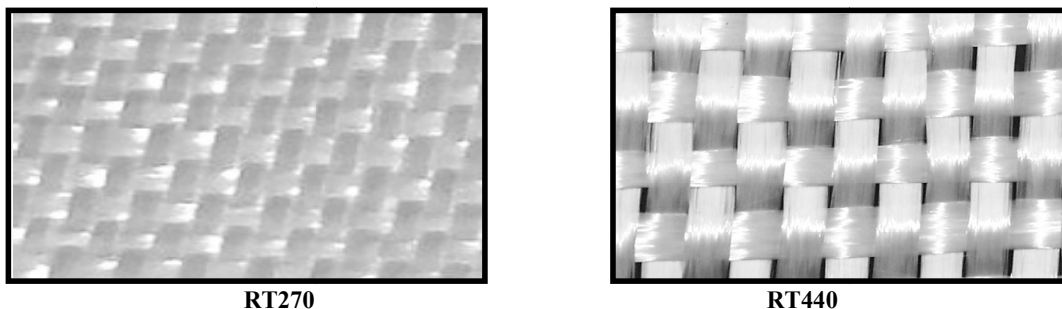


Fig. 1 Woven fabrics

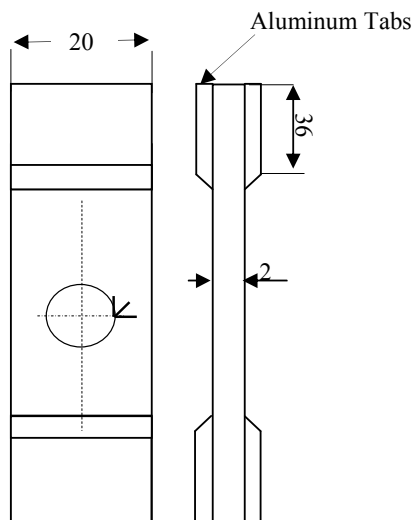


Fig. 2 Tensile specimen

IV. TENSILE FRACTURE TEST

For the tensile fracture test, five specimens of each material were tested according to ASTM D3039 using an Instron machine at a constant loading rate of 0.5 mm/min.

Fig. 3 shows the specimen after the test. Table I presents the real limit and a coded value of the influents parameters.

Taking into account of all influent parameters, the experiment of type 2³.3¹ was chosen. Because of the units diversity, values were coded by the relation [7]:

$$X_i = (x_i - x_{i0}) / \Delta x_i \quad (1)$$

Table II shows the coded influent parameters.

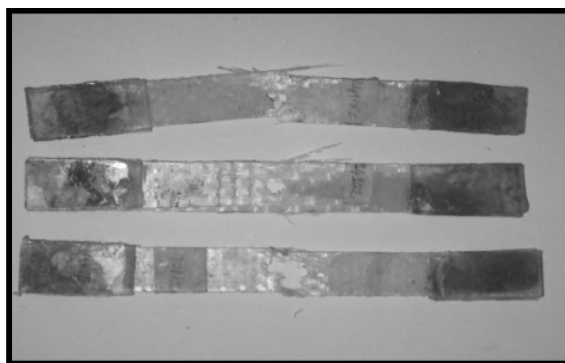


Fig. 3 Photograph showing the critical damage zone formed on laminated specimen

TABLE I
PARAMETERS VARIATIONS

INDEPENDENT VARIABLES		UNIT	SUPERIOR LEVEL	INTERMEDIATE LEVEL	INFERIOR LEVEL
MATERIALS (WEAVING TYPES)	X1 (X1)		Rt440 (+1)		Rt270 (-1)
NOTCH DIAMETER	X2 (X2)	[MM]	4 (+1)	3 (0)	2 (-1)
PRECRACK LENGTH	X3 (X3)	[MM]	3 (+1)	2 (0)	1 (-1)
PRECRACK ORIENTATION ANGLE	X4 (X4)	[°]	90 (+1)	45 (0)	0 (-1)
MAXIMUM TENSILE LOAD	Y (X1,β1)	[N]	OUTPUT PARAMETERS		

TABLE II
EXPERIMENTAL DESIGN OF THE TYPE 2³.3¹

Nº	X1	X2	X3	X4	X1 X2	X1 X3	X1 X4	X2 X3	X2 X4	X3 X4	X1 X2 X3	X1 X2 X4	X1 X3 X4	X2 X3 X4	X4*	\bar{Y}
1	-	-	-	-	+	+	+	+	+	+	-	-	-	-	1/3	7885
2	+	-	-	0	-	-	0	+	0	0	+	0	0	0	-2/3	8595
3	-	+	-	+	-	+	-	-	+	-	+	-	+	-	1/3	9085
4	+	+	-	-	+	-	-	-	-	+	-	-	+	+	1/3	7785
5	-	-	+	0	+	-	0	-	0	0	+	0	0	0	-2/3	8090
6	+	-	+	+	-	+	+	-	-	+	-	-	+	-	1/3	9960
7	-	+	+	-	-	-	+	+	-	-	-	+	+	-	1/3	7725
8	+	+	+	0	+	+	0	+	0	0	+	0	0	0	-2/3	7865
9	-	-	-	+	+	+	-	+	-	-	-	+	+	+	1/3	9545
10	+	-	-	-	-	-	-	+	+	+	+	+	+	-	1/3	8390
11	-	+	-	0	-	+	0	-	0	0	+	0	0	0	-2/3	7785
12	+	+	-	+	+	-	+	-	+	-	-	+	-	-	1/3	9335
13	-	-	+	-	+	-	+	-	+	-	+	-	+	+	1/3	7780
14	+	-	+	0	-	+	0	-	0	0	-	0	0	0	-2/3	8350
15	-	+	+	+	-	-	-	+	+	+	-	-	-	+	1/3	8955
16	+	+	+	-	+	+	-	+	-	-	+	-	-	-	1/3	7765
17	-	-	-	0	+	+	0	+	0	0	-	0	0	0	-2/3	8635
18	+	-	-	+	-	-	+	+	-	-	+	-	-	+	1/3	10040
19	-	+	-	-	-	+	+	-	-	+	+	+	-	+	1/3	7750
20	+	+	-	0	+	-	0	-	0	0	-	0	0	0	-2/3	8025
21	-	-	+	+	+	-	-	-	-	+	+	+	-	-	1/3	9300
22	+	-	+	-	-	+	-	-	+	-	-	+	-	+	1/3	8060
23	-	+	+	0	-	-	0	+	0	0	-	0	0	0	-2/3	7735
24	+	+	+	+	+	+	0	+	+	+	+	+	+	+	1/3	9030

V.RESULTS AND INTERPRETATIONS

Using the regression analysis of [7]-[10], we obtain the regression coefficients:

$$\bar{Y} = \sum_1^N X_0 Y / \sum_1^N X_0^2 \tag{2}$$

$$\beta_u = \sum_1^N X_i^* \bar{Y} / \sum_1^N X_i^{*2} \tag{3}$$

$$\beta_0 = \bar{Y} - (1/C^*) \sum_1^k \beta_u \tag{4}$$

$$X_4^* = X_4^2 - (2/3) \tag{5}$$

$\beta_0 = 8134.87$; $\beta_1 = 122.08$; $\beta_2 = 241.25$; $\beta_3 = 93.33$; $\beta_4 = 756.87$; $\beta_{12} = -57.92$; $\beta_{13} = -1.67$; $\beta_{14} = 38.75$; $\beta_{23} = 35.83$; $\beta_{24} = -84.37$; $\beta_{34} = -17.5$; $\beta_{123} = -21.66$; $\beta_{124} = -7.5$; $\beta_{134} = 13.13$; $\beta_{234} = -31.25$; $\beta_{44} = 514.69$

The confidence interval ($|\Delta\beta_i| = S(\beta_i).t_{\alpha, fy}$) of the regression coefficients obtained with $\alpha = 0.05$ and 24 experiments is equal to 51.21 [8].

With: $t(0.05, 24) = 1.711$ and $S(\beta_i) = 29.93$

Taking only the significant coefficients, the model can be written as follows:

$$Y(X_i, \beta_i) = 7791.74 + 122.08X_1 + 241.25X_2 + 93.33X_3 + 756.87X_4 - 57.92X_1X_2 - 84.37X_2X_4 + 514.69X_4^2 \tag{6}$$

The model presented by (6) describes the phenomenon adequately by the fact that $F_{exp.} = 1.287$ is lower than $F_{th.} = 2.11$ [7].

In order to obtain the graphical representation of (2), we maintain the type of weaving fibers (X1) and the notch diameter (X2= 3mm average value), the mathematical model presented in (2) has the form:

$$Y(X_i, \beta_i) = 7791.74 + 93.33X_3 + 756.87X_4 + 514.69X_4^2 \tag{7}$$

The graphical representation of (7) is given in Fig. 4.

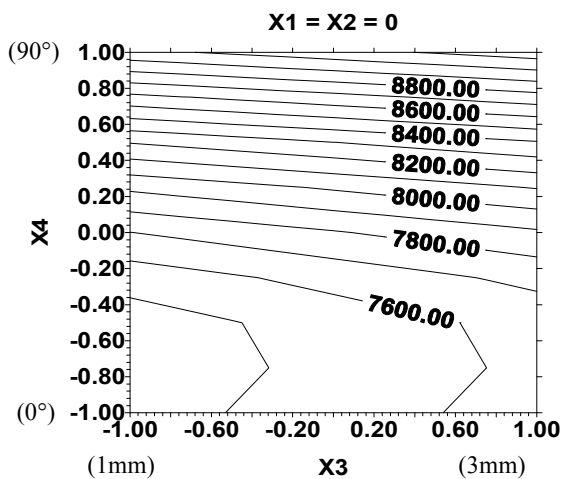


Fig. 4 Effect of the precrack length and the angle of orientation on the maximum load

For an increase in a precrack length, the maximum tensile load does not increase linearly with respect to the angle of orientation from 0 to 10.8° because the direction of the traction charge is perpendicular with respect to the length axis of the crack which provides a weak resistance against the breakdown of break [11]. Up to this value, the load does not increase linearly from 10.8 to 45° because the structure of fibers that stop the progress of fracture [12], and then increases linearly and break rapidly from 45 to 90° because the crack axis is parallel to the charge axis [13].

The angle 10.8° was calculated from (1):

$$x_i = X_i * \Delta x + x_{i0} ;$$

(where $\Delta x = x_i - x_{i0} = 0.76 * 45 + 45$)

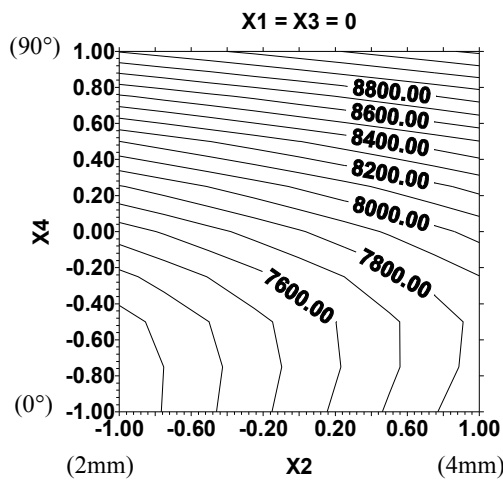


Fig. 5 Effect of the notch diameter and the angle of orientation on the maximum loading

From Fig. 4, the maximum load 9650 N was reached for an orientation angle of 90° and a precrack length of 3mm for a central notch diameter of 3mm.

In the second stage, we maintain the type of weaving X1 and the precrack length X3 (2mm average value), the model described in (2) takes the form:

$$Y(X_i, \beta_i) = 7791.74 + 241.25X_2 + 756.87X_4 - 84.37X_2X_4 + 514.69X_4^2 \quad (8)$$

Equation (4) is represented in Fig. 5. With an increase in the notch diameter, the maximum tensile fracture does not decrease linearly but slowly with the growth of the angle of orientation from 0 to 21.6°. The load increases in a non-linear way and slowly for an angle ranging from 21.6° to 66.6°. Beyond this value, it increases linearly and rapidly (Fig. 5), because the material is insensitive to the notch effect. It even shows the opposite effect, namely that the ligament is much stronger resistant than the depth of cut is large. This can be explained by the mechanisms of damage at the mesoscopic scale of oblique folds [14], [15].

In the third stage, we maintain the type of weaving X1 and the angle of orientation X4 (45° average value), the model presented in (6) becomes:

$$Y(X_i, \beta_i) = 7791.74 + 241.25X_2 + 93.33X_3 \quad (9)$$

Equation (9) is represented in Fig. 6.

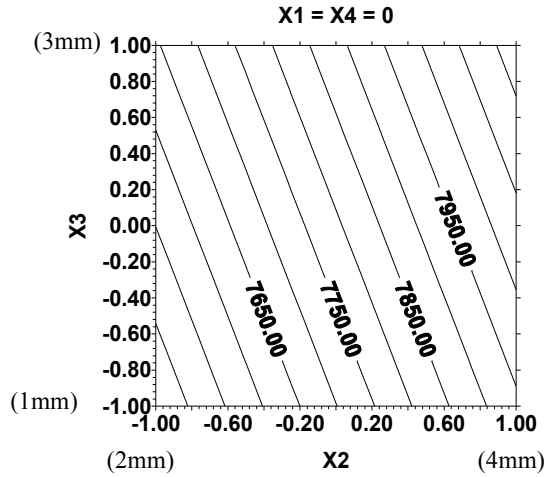


Fig. 6 Effect of the notch diameter and the precrack length on the maximum load

From Fig. 6, we note that the simultaneous increase of the notch diameter (X2) and the precrack length (X3) generate a linear growth of the maximum loading tensile [16]-[18].

For the fourth stage, we maintain the notch diameter X2 (3mm average value) and X3 (2mm average value), (6) takes the form:

$$Y(X_i, \beta_i) = 7791.74 + 122.08X_1 + 756.87X_4 + 514.69X_4^2 \quad (10)$$

Fig. 7 shows the mathematical representation of (10).

From Fig. 7, the change in the type of weaving fibers generates no linear decrease in the maximum load with the variation in the angle of orientation from 0° to 10.8°. The load increases in a non linear way and slowly for an angle ranging from 10.8° to 59.4°, then linearly and rapidly for an angle ranging from 59.4° to 90° [19]-[21].

In the fifth stage, the notch diameter and the angle of orientation are maintained to their average values $X_2 = 3\text{mm}$ and $X_4 = 45^\circ$, (6) takes the form:

$$Y(X_i, \beta_i) = 7791.74 + 122.08X_1 + 93.33X_3 \quad (11)$$

The maximum load given by (11) is represented in Fig. 8. It is noted that the maximum load increases linearly with the variation of the type of weaving and the precrack length [22].

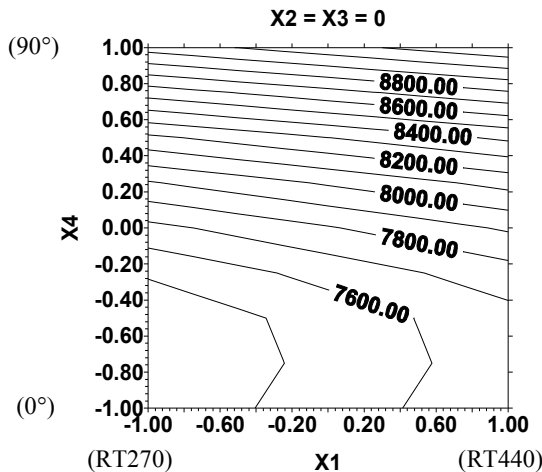


Fig. 7 Effect of the weaving type and the angle of orientation on the maximum load

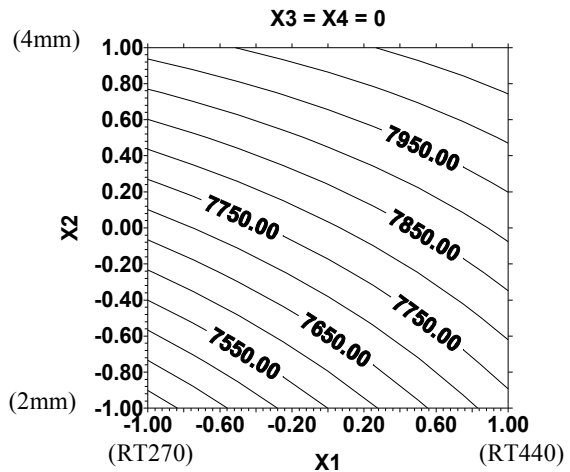


Fig. 9 Effect of the weaving type and the notch diameter on the maximum loading

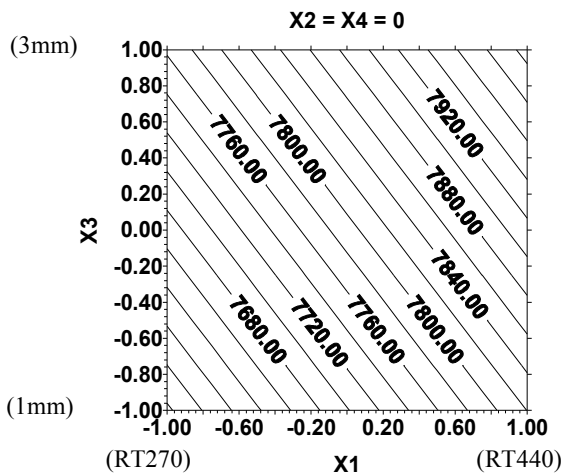


Fig. 8 Effect of material and the crack length on the maximum loading

In the last stage, we maintain the precrack length ($X_3 = 2\text{mm}$) and the angle of orientation $X_4 = 45^\circ$ to their average values, (6) becomes:

$$Y(X_i, \beta_i) = 7791.74 + 122.08X_1 + 241.25X_2 - 57.92X_1X_2 \quad (12)$$

Fig. 9 shows the mathematical representation of (12).

Fig. 9 shows that the maximal load in the case of RT440 is higher than that of RT270 because the resistance of the former (1,100 N/cm) is higher than that of the latter (360 N/cm) in traction [23], [24].

The same figure also shows that the load increases with the notch diameter growth [25], [26].

VI. CONCLUSION

The tensile fracture test is carried out in order to determine the maximum fracture load of two woven fabric unsaturated poly-ester matrix reinforced with glass fibers. The circular central notches of different diameters are drilled. For each diameter the artificial precracks are made. The precracks have different orientations. By applying the planning experimental design, a mathematical model gives the maximum tensile load is obtained. It takes into account the different parameters like notch diameter, the precrack length, the angle of orientation and the type of weaving. From the obtained results, the tensile load for a material RT270 is lower than that of material RT440. The load increases linearly with the simultaneous increase of the notch diameter and the precrack length. On the other hand it decreases with the increase of the orientation angle of the precrack and the notch diameter.

ACKNOWLEDGMENT

This work is in the framework of project "CNEPRU," Characterization of the mechanical properties of composite materials, experimental and numerical modeling; code (J0306220110007).

REFERENCES

- [1] Ouinas D, Serier B and Bouiadja B. Interaction d'une fissure émanant d'entaille semi-circulaire orientée perpendiculairement à l'interface céramique/métal. *J. Revue des composites et des matériaux avancés* 2005; 5: 221-244.
- [2] Naik NK, Shembeker PS. Notched strength of fabric laminates I: prediction. *J.Comp Sci & Technol* 1992; 44:1-12.
- [3] Xiao J, Bathias C. Modified tan's model for the strength prediction of woven laminates with circular holes. *J.Comp Eng* 1993; 3: 961-973.
- [4] Kim JK, Kim DS, Takeda N. Notched strength and fracture criterion in fabric composites containing a circular hole. *J. Comp Mater* 1995; 29: 982-998.
- [5] Ashbee K.H.G and Wyatt R.C. Water damage in glass fiber-resin composites. *Proc.R.Soc .London*; 1969, A312, p. 553-564.
- [6] ASTM 2004. Standard Test Method for Tensile Properties of Polymer Matrix Composite Materials. D3039/D3039M; edition 2004.
- [7] Scheffler E. Einführung in die Praxis der statistischen Versuchsplanung. VEB deutscher Verlag für Grundstoffindustrie. Leipzig; 1986.

- [8] Nalimov V. P., Tschernova N. A. *Statistichieski Methodi Planirovania Extremalnack Experimentov*. Naouka Moscou; 1965.
- [9] Vivier S. *Stratégie d'optimisation par la méthode des plans d'expériences et application aux dispositifs électroniques modélisés par éléments finis*. Thèse de Doctorat. Ecole centrale de Lille; 2002.
- [10] Hebbar A. *Méthodes statistiques de planification extrême des expériences*, Polycoipié. Université de Mostaganem; 2006.
- [11] Srinivas M., Kamat S.V. and Rama Rao P. Influence of mixed mode I/III loading on the fracture toughness of mild steel at various strain rates. *J. Materials Science and Technology* 2004; 20: 235-242.
- [12] Luhowiak W. et Collot C. Influence du diamètre des bulles sur la microfissuration d'un joint collé. *J. Materials and Structures* 2006; 19: 127-32.
- [13] Chan K.S and Cruse T.A. Stress intensity factors for anisotropic compact-tension specimens with inclined cracks. *J. Engineering Fracture Mechanics* 1986; 23: 863-874
- [14] Tallaron C, Rousy D. *Thermomechanical behaviour under static and cyclic loading, of multidirectionnal laminated C/C composites materials, with or without notches*. Institut national des sciences appliquées de Lyon. Travaux Universitaires, Villeurbanne, France; 1996.
- [15] Weiju R and Theodore N. Notch size effects on high cycle fatigue limit stress of Udimet 720. *J. Materials Science and Engineering A* 2003; 357: 41-152.
- [16] Lukás P, Kunz L, Weiss B, Stickler R. Notch Size Effect In Fatigue. *J. Fatigue & Fracture of Engineering Materials & Structures* 2007; 12: 3175 -186.
- [17] Akourri O, Louah M, Kifani A, Gilgert G. and Pluvinage G. The effect of notch radius on fracture toughness JIc. *J. Engineering Fracture Mechanics* 2000; 65: 491-505.
- [18] Zhou B, Kokin K. Effect of surface pre-crack morphology on the fracture of thermal barrier coatings under thermal shock. *J. Acta Materialia* 2004; 52: 4189-4197.
- [19] Naghipour P, Bartsch M, Chernova L, Hausmann J and Voggenreiter H. Effect of fiber angle orientation and stacking sequence on mixed mode fracture toughness of carbon fiber reinforced plastics: Numerical and experimental investigations. *J. Materials Science and Engineering:A* 2010; 527: 3509-517.
- [20] Wood M.D.K, Sun X, Tong L, Katzos A, Rispler, A.R. The Effect of Stitch distribution on Mode I delamination toughness of stitched laminated composites– experimental results and fea simulation. *J. Composites Science and Technology* 2007; 67: 1058-1072.
- [21] Luhowiak W et Collot C. Influence du diamètre des bulles sur la microfissuration d'un joint collé. *J. Materials and Structures* 2006; 19: 27-32.
- [22] Xu S, Shen G and Tyson W.R. Effect of crack-tip plasticity on crack length estimation methods for SENB sample. *Engineering Fracture Mechanics*; 2005, p.1454-1459.
- [23] Wen-Shyong K, Tse-Hao K and Cheng-Po C. Effect of weaving processes on compressive behavior of 3D woven composites. *J. Composites Part A: Applied Science and Manufacturing* 2007; 38: 555-565.
- [24] Documentations A.N.G.I S.R.L, Commercial offices and warehouse 14018 Villafranca d'Asti, Italie, angi@angisrl.com
- [25] Swanson R. E, Thompson A. W. and Bernstein I. M. Effect of notch root radius on stress intensity in mode I and mode III loading. *J. Metallurgical and Materials Transactions A* 2007; 17: 1633-1637.
- [26] Mohamed K, Kaleemulla A and Siddeswarappa B. Effect of notch size and fibre content on the tensile strength of fabric reinforced hybrid composites. *J. International Journal of Materials and Product Technology* 2008; 31: 283 – 292.